

Article

# The Structural and Dielectric Properties of $\text{Bi}_{3-x}\text{Nd}_x\text{Ti}_{1.5}\text{W}_{0.5}\text{O}_9$ ( $x = 0.25, 0.5, 0.75, 1.0$ )

Sergei V. Zubkov <sup>1,\*</sup>, Ivan A. Parinov <sup>2,\*</sup> and Yulia A. Kuprina <sup>1,\*</sup><sup>1</sup> Research Institute of Physics, Southern Federal University, Stachki Ave., 194, 344090 Rostov-on-Don, Russia<sup>2</sup> I. I. Vorovich Mathematics, Mechanics and Computer Sciences Institute, Southern Federal University, 344090 Rostov-on-Don, Russia

\* Correspondence: svzubkov61@mail.ru (S.V.Z.); parinov\_ia@mail.ru (I.A.P.); kyprins@rambler.ru (Y.A.K.)

**Abstract:** A new series of layered perovskite-like oxides  $\text{Bi}_{3-x}\text{Nd}_x\text{Ti}_{1.5}\text{W}_{0.5}\text{O}_9$  ( $x = 0.25, 0.5, 0.75, 1.0$ ) was synthesized by the method of high-temperature solid-state reaction, in which partial substitution of bismuth (Bi) atoms in the dodecahedra of the perovskite layer (*A*-positions) by Nd atoms takes place. X-ray structural studies have shown that all compounds are single-phase and have the structure of Aurivillius phases (APs), with close parameters of orthorhombic unit cells corresponding to space group  $A2_1am$ . The dependences of the relative permittivity  $\epsilon/\epsilon_0$  and the tangent of loss  $\text{tg}\sigma$  at different frequencies on temperature were measured. The piezoelectric constant  $d_{33}$  was measured for  $\text{Bi}_{3-x}\text{Nd}_x\text{Ti}_{1.5}\text{W}_{0.5}\text{O}_9$  ( $x = 0.25, 0.5, 0.75$ ) compounds of the synthesized series.

**Keywords:** Aurivillius phases;  $\text{Bi}_{3-x}\text{Nd}_x\text{Ti}_{1.5}\text{W}_{0.5}\text{O}_9$ ; activation energy  $E_a$ ; Curie temperature  $T_C$



**Citation:** Zubkov, S.V.; Parinov, I.A.; Kuprina, Y.A. The Structural and Dielectric Properties of  $\text{Bi}_{3-x}\text{Nd}_x\text{Ti}_{1.5}\text{W}_{0.5}\text{O}_9$  ( $x = 0.25, 0.5, 0.75, 1.0$ ). *Electronics* **2022**, *11*, 277. <https://doi.org/10.3390/electronics11020277>

Academic Editors: Tamás Orosz, David Pánek, Anton Rassólkin and Miklos Kuczmann

Received: 8 December 2021

Accepted: 13 January 2022

Published: 16 January 2022

**Publisher's Note:** MDPI stays neutral with regard to jurisdictional claims in published maps and institutional affiliations.



**Copyright:** © 2022 by the authors. Licensee MDPI, Basel, Switzerland. This article is an open access article distributed under the terms and conditions of the Creative Commons Attribution (CC BY) license (<https://creativecommons.org/licenses/by/4.0/>).

## 1. Introduction

In 1949, while studying the  $\text{Bi}_2\text{O}_3\text{-TiO}_2$  system, V. Aurivillius established the formation of an oxide:  $\text{Bi}_4\text{Ti}_3\text{O}_{12}$  with a perovskite-type structure [1]. Then, within two years, he obtained several more oxides with a similar structure [2,3]. However, at the first stage, V. Aurivillius limited himself to studying only the structure of the compounds obtained. Only ten years later G. Smolenskiy, V. Isupov and A. Agranovskaya [4] discovered the ferroelectric properties of  $\text{Bi}_2\text{PbNbO}_9$ , which belongs to this class of compounds. Subsequently, several tens of Aurivillius phases were obtained, and almost all of them turned out to be ferroelectrics [5–10]. Aurivillius phases (APs) form a large family of bismuth-containing layered perovskite type compounds, with the chemical composition described by the general formula  $A_{m-1}\text{Bi}_2\text{B}_m\text{O}_{3m+3}$ . The crystal structure of the APs consists of alternating  $[\text{Bi}_2\text{O}_2]^{2+}$  layers separated by  $m$  perovskite-like layers  $[\text{A}_{m-1}\text{B}_m\text{O}_{3m+1}]^{2-}$ , where  $A$  are ions with large radii ( $\text{Bi}^{3+}$ ,  $\text{Ca}^{2+}$ ,  $\text{Gd}^{3+}$ ,  $\text{Sr}^{2+}$ ,  $\text{Ba}^{2+}$ ,  $\text{Pb}^{2+}$ ,  $\text{Na}^+$ ,  $\text{K}^+$ ,  $\text{Y}^{3+}$ ,  $\text{Ln}^{3+}$  (lanthanides)) and have dodecahedral coordination, while the  $B$ -positions inside oxygen octahedra are occupied by strongly charged ( $\geq 3^+$ ) cations with a small radius ( $\text{Ti}^{4+}$ ,  $\text{Nb}^{5+}$ ,  $\text{Ta}^{5+}$ ,  $\text{W}^{6+}$ ,  $\text{Mo}^{6+}$ ,  $\text{Fe}^{3+}$ ,  $\text{Mn}^{4+}$ ,  $\text{Cr}^{3+}$ ,  $\text{Ga}^{3+}$ , etc.). The value of  $m$  is determined by the number of perovskite layers  $[\text{A}_{m-1}\text{B}_m\text{O}_{3m+1}]^{2-}$  located between the fluorite-like layers  $[\text{Bi}_2\text{O}_2]^{2+}$  and can take integer or half-integer values in the range 1–5 (Figure 1).

If  $m$  is a half-integer number, then in the lattice, there are alternative perovskite layers with  $m$  differing by 1. For example, at  $m = 1.5$ , the lattice has an equal number of layers with  $m = 1$  and  $m = 2$ . The value  $m = 1$  corresponds, for example, to the compound  $\text{Bi}_2\text{WO}_6$ ,  $m = 2$  corresponds to  $\text{Bi}_2\text{PbNbO}_9$ ,  $m = 3$  corresponds to  $\text{Bi}_4\text{Ti}_3\text{O}_{12}$ ,  $m = 4$  corresponds to  $\text{Bi}_4\text{CaTi}_4\text{O}_{15}$ ,  $m = 5$  corresponds to  $\text{Bi}_4\text{Sr}_2\text{Ti}_5\text{O}_{18}$ .

Positions  $A$  and  $B$  can be occupied by the same or by several different atoms. Atomic substitutions in positions  $A$  and  $B$  have a significant effect on the electrophysical characteristics of the APs. In particular, there are large changes in the values of dielectric constants, conductivity. Moreover, Curie temperature  $T_C$  can also vary within wide limits. Thus, the

study of cation-substituted APs plays an important role in the creation of materials for various technological applications.

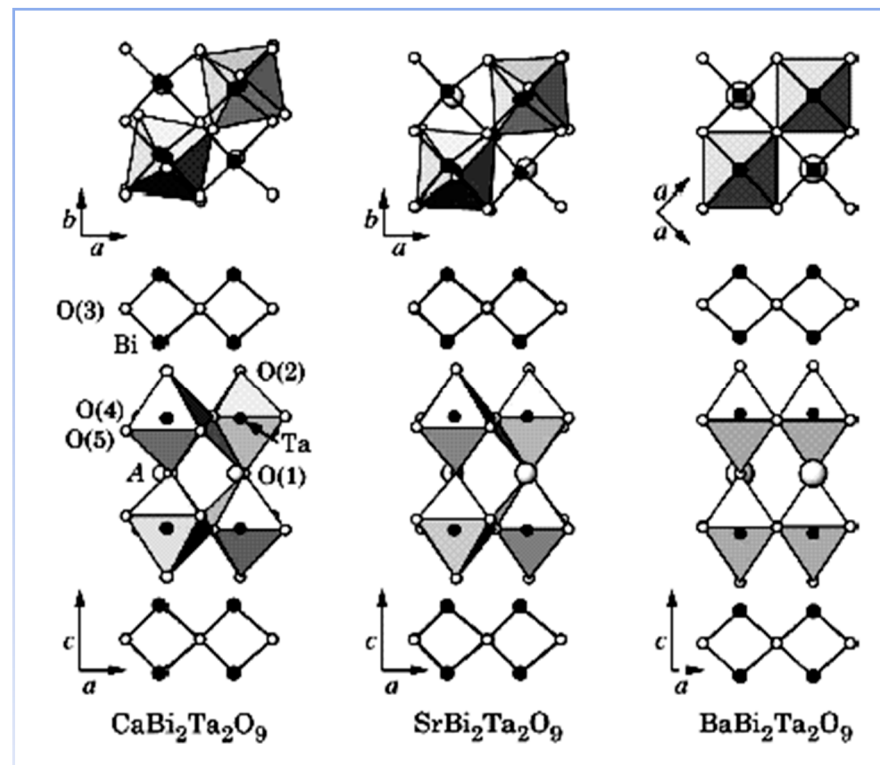


**Figure 1.** Crystal structure of  $ABi_2Ta_2O_9$ , where  $A = Ca, Sr, Ba$ .

The structure of  $Bi_2A_{m-1}B_mO_{3m+3}$  compounds above the Curie point  $T_C$  is tetragonal and belongs to the space group  $I4/mmm$ . The type of space group below the Curie point  $T_C$  depends on the value of the number  $m$ . For odd  $m$ , the space group of the ferroelectric phase is  $B2cb$  or  $Pca2_1$ , for even  $m$ , it is  $A2_1am$ , and for half-integer  $m$ , it is  $Cmm2$  or  $I2cm$ .

This work considers the conditions for the existence of these compounds [11]:

$$t_1 < t = \left[ (1.12R_A + R_O) / \sqrt{2}(R_B + R_O) \right] < t_2, \quad (1)$$

where  $R_A, R_B$  are the cation radii,  $R_O$  is the oxygen anion radius,  $t$  is the Goldschmidt tolerance factor. The boundary values of the tolerance factor, which determines the possibility of the existence of a compound belonging to the APs, are defined as  $t_1 = 0.870$  and  $t_2 = 0.985$ . A detailed study of the regularities of changes in the Curie temperature of the Aurivillius phases on such parameters as the radii and electronegativity of the  $A$ - and  $B$ -cations, as well as on the cell parameters, was carried out in [12]. Some anomalies in the properties of layered ferroelectrics  $A_{m-1}Bi_2B_mO_{3m+3}$  were also considered [13]. In particular, it was shown that  $Bi_2O_2$  layers have a constricting effect on the layered structure of these compounds, but the strength of such an effect decreases with an increase in the number of perovskite layers. Moreover, it was shown that the Curie temperatures pass through a maximum with increasing distortions of the pseudoperovskite cell in the perovskite-like layer, and the position of the maximum changes with a change in the number of perovskite layers  $m$ . Despite the fact that the crystal structure of the APs has been fairly well studied by various methods (X-ray powder diffraction, neutron diffraction, etc.), some aspects related to the distortion of the APs' unit cell from the "ideal" tetragonal system with the space group  $I4/mmm(139)$ , and the reasons for such distortions, are of scientific interest. The structural features of APs, which determine the appearance of ferroelectric properties in these compounds, have also not been sufficiently clarified. Basically, this is attributed to the

displacement of the *B*-ion ( $\text{Ti}^{4+}$ ,  $\text{Nb}^{5+}$ ,  $\text{Ta}^{5+}$ ) from the center of the oxygen octahedron in the perovskite layers. Scientific interest in the synthesis and study of new APs is stimulated by numerous examples of their use in various electronic devices, due to their unique physical properties (piezoelectric, ferroelectric, etc.). They demonstrate low temperature coefficients of dielectric and piezoelectric losses, and low aging temperatures in addition to high Curie temperatures ( $T_C \leq 965 \text{ }^\circ\text{C}$ ) [14,15].

In recent years, more attention has been placed on the design and studies of new APs [16–20]. The APs, such as  $\text{SrBi}_2\text{Nb}_2\text{O}_9$  (SBN),  $\text{SrBi}_4\text{Ti}_4\text{O}_{15}$  (SBTi),  $\text{SrBi}_2\text{Ta}_2\text{O}_9$  (SBTa),  $\text{La}_{0.75}\text{Bi}_{3.25}\text{Ti}_3\text{O}_{12}$  (BLT) and so on, were accepted as excellent materials for the energy independent ferroelectric memory with small access time (FeRAM) [21–25].  $\text{Bi}_3\text{TiNbO}_9$  (BTNO) with  $m = 2$  that consists of  $(\text{Bi}_2\text{O}_2)^{2+}$  layers between which there are  $(\text{BiTiNbO}_7)^{2-}$  layers [26] is a promising material for fabricating high temperature piezoelectric sensors because of their very high Curie temperature  $T_C$  (914–921  $^\circ\text{C}$ ) [14,15], despite the fact that the piezoelectric modulus of BTNO ceramic is fairly low ( $d_{33} < 7 \text{ pC/N}$ ) [27]. Numerous examples [28–42] showed that replacements of atoms in *A*- and also in *B*-positions of an AP's crystal lattice led to a change in the structure, the dielectric properties and significantly influenced the polarization processes in these compounds.

The purpose of this study was to investigate the dielectric characteristics when bismuth cation (*A*-position) is replaced by neodymium ions of the basic composition  $\text{Bi}_3\text{Ti}_{1.5}\text{W}_{0.5}\text{O}_9$ . It was previously observed that the partial replacement of bismuth ions by neodymium cations in the series of perovskite-like Bi-containing oxides  $\text{Bi}_3\text{TiNbO}_9$ ,  $\text{Bi}_3\text{TiTaO}_9$  led to a significant decrease in the phase transition temperature (Curie temperature  $T_C$ ) and a change in dielectric properties [43].

## 2. Experimental Section

Polycrystalline samples of APs were synthesized by the solid-phase reaction of the corresponding  $\text{Bi}_2\text{O}_3$ ,  $\text{TiO}_2$ ,  $\text{Nd}_2\text{O}_3$ ,  $\text{WO}_3$ . After weighting in accordance with the stoichiometric composition and a thorough grinding of the initial compounds with the addition of ethyl alcohol, the pressed samples were calcined at a temperature of 770  $^\circ\text{C}$  for 2 h. The samples were fired in a laboratory muffle furnace in air. Then, the samples were repeatedly ground and pressed into pellets with a diameter of 10 mm and a thickness of 1.0–1.5 mm, followed by the final synthesis of APs at a temperature of 1100  $^\circ\text{C}$  (for 2 h).

The X-ray diffraction patterns were recorded on a DRON-3M diffractometer with attachment for powder diffraction and an X-ray tube BSV21-Cu with a Cu X-ray tube. The Cu  $K_{\alpha 1, \alpha 2}$  radiation was separated from the total spectrum with the use of a Ni-filter. The X-ray diffraction patterns were measured in the range of  $2\theta$  angles from 10 $^\circ$  to 65 $^\circ$  with a scan step of 0.02 $^\circ$  and an exposure (intensity registration time) of 4 s per point. The analysis of the profiles of the diffraction patterns, the determination of the positions of the lines, their indexing (*hkl*), and the refinement of the unit cell parameters were performed by using the PCW 2.4 program [44]. For dielectric permittivity and electrical conductivity measurements, on flat surfaces of samples of APs, in the form of disks with a diameter of 10 mm and a thickness of approximately 1 mm, electrodes were deposited, using an Ag-paste annealed at a temperature of 700  $^\circ\text{C}$  (for 1 h). The temperature and frequency dependences of the dielectric characteristics were measured using an E7-20 immittance meter in the frequency range from 100 kHz to 1 MHz and at temperatures in the range from room temperature to 900  $^\circ\text{C}$ . All the samples were poled in an oil bath at 125  $^\circ\text{C}$  under 35 kV/cm for 30 min.

## 3. Results and Discussion

Powder X-ray diffraction patterns of all investigated solid solutions  $\text{Bi}_{3-x}\text{Nd}_x\text{Ti}_{1.5}\text{W}_{0.5}\text{O}_9$  ( $x = 0.25, 0.5, 0.75, 1.0$ ) correspond to single-phase APs with  $m = 2$ , and do not contain additional reflections isostructural to the known perovskite-like oxide  $\text{Bi}_3\text{Ti}_{1.5}\text{W}_{0.5}\text{O}_9$ . It was found that all synthesized APs crystallize in an orthorhombic system with a unit cell space group  $A2_1am(36)$ . The diffraction patterns of all the compounds correspond to the

APs with  $m = 2$ . Figure 2 shows the experimental powder X-ray diffraction patterns of the studied compounds.

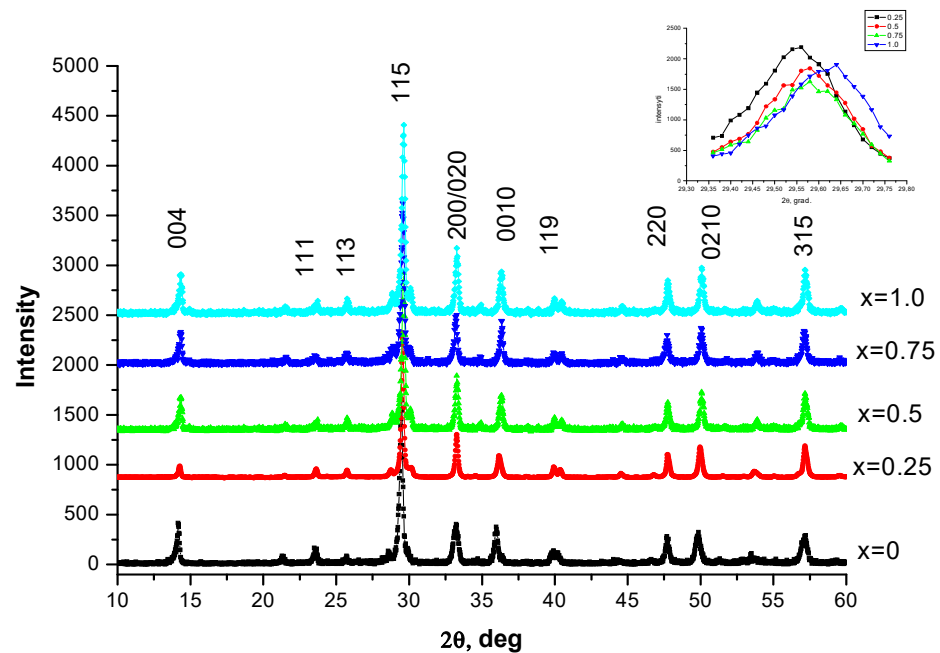


**Figure 2.** Experimental curve of the X-ray powder diffraction patterns of the  $\text{Bi}_{3-x}\text{Nd}_x\text{Ti}_{1.5}\text{W}_{0.5}\text{O}_9$  ( $x = 0.0, 0.25, 0.5, 0.75, 1.0$ ) compounds.

According to the data of X-ray diffraction, the parameters of the unit cell and the volume of the unit cell were determined; they are given in Table 1.

**Table 1.** Unit cell parameters  $a_0$ ,  $b_0$ ,  $c_0$ ,  $V$ ,  $a_t$  is the parameter of the tetragonal period,  $c'$  is the octahedron height along axis  $c$ ,  $\delta c'$  is the deviation of the unit from the cubic shape,  $\delta b$  is the rhombic distortion.

Compounds	$a_0, \text{\AA}$	$b_0, \text{\AA}$	$c_0, \text{\AA}$	$V, \text{\AA}^3$	$c', \text{\AA}$	$a_t, \%$	$\delta c', \%$	$\delta b_0, \%$
$\text{Bi}_{2.75}\text{Nd}_{0.25}\text{Ti}_{1.5}\text{W}_{0.5}\text{O}_9$	5.3861	5.3742	24.8572	719.51	3.7586	3.8043	−1.2	−0.2
$\text{Bi}_{2.5}\text{Nd}_{0.5}\text{Ti}_{1.5}\text{W}_{0.5}\text{O}_9$	5.3916	5.3742	24.8421	719.81	3.7263	3.8063	−2.1	−0.3
$\text{Bi}_{2.25}\text{Nd}_{0.75}\text{Ti}_{1.5}\text{W}_{0.5}\text{O}_9$	5.3977	5.3875	24.8388	722.31	3.7258	3.8131	−2.28	−0.18
$\text{Bi}_2\text{NdTi}_{1.5}\text{W}_{0.5}\text{O}_9$	5.4013	5.3903	24.8388	723.17	3.7248	3.8154	−2.28	−0.2

Table 1 also shows the parameters of the orthorhombic  $\delta b_0$  and tetragonal  $\delta c'$  deformation; average tetragonal period  $a_t$ , coefficient of tolerance  $t$  and the average thickness of one perovskite layer  $c'$ ;  $c' = 3c_0/(8 + 6m)$  is the thickness of a single perovskite-like layer,  $m$  is the number of layers,  $a_t = (a_0 - b_0)/2\sqrt{2}$  is the average value of the tetragonal period,  $a_0, b_0, c_0$  are the lattice periods,  $\delta c' = (c' - a_t)/a_t$  is the deviation of a cell from a cubic shape, that is a lengthening or shortening from a cubic shape,  $\delta b_0 = (b_0 - a_0)/a_0$  is the rhombic deformation. The obtained unit cell parameters of the studied APs  $\text{Bi}_{3-x}\text{Nd}_x\text{Ti}_{1.5}\text{W}_{0.5}\text{O}_9$  samples ( $x = 0.25, 0.5, 0.75, 1.0$ ) are close to those determined earlier:  $a = 5.4018$  (2)  $\text{\AA}$ ,  $b = 5.3727$  (4)  $\text{\AA}$ ,  $c = 24.9388$  (1)  $\text{\AA}$  [23]. In order to obtain the degree of distortion of the ideal structure of perovskite in  $\text{Nd}^{3+}$ , we determined the tolerance factor  $t$ , which is presented in Table 2.

**Table 2.** Dielectric characteristics of  $\text{Bi}_{3-x}\text{Nd}_x\text{Ti}_{1.5}\text{W}_{0.5}\text{O}_9$  ( $x = 0.25, 0.5, 0.75, 1.0$ ): Curie temperature  $T_C$ , piezomodule  $d_{33}$ , tolerance factor  $t$ , relative permittivity  $\epsilon/\epsilon_0$ , activation energy  $E_n$ .

Compounds	$T_C, ^\circ\text{C}$	$d_{33}, \text{pC/N}$	$t$	$\epsilon/\epsilon_0(T)$ (at 100 kHz)	$E_1/E_2/E_3, \text{eV}$
$\text{Bi}_{2.75}\text{Nd}_{0.25}\text{Ti}_{1.5}\text{W}_{0.5}\text{O}_9$	681	10	0.9778	1000	0.67/0.29/0.06
$\text{Bi}_{2.5}\text{Nd}_{0.5}\text{Ti}_{1.5}\text{W}_{0.5}\text{O}_9$	637	5	0.9745	500	0.77/0.31/0.1
$\text{Bi}_{2.25}\text{Nd}_{0.75}\text{Ti}_{1.5}\text{W}_{0.5}\text{O}_9$	617	3.5	0.9713	550	0.65/0.21
$\text{Bi}_2\text{NdTi}_{1.5}\text{W}_{0.5}\text{O}_9$	165	0	0.9681	160	-

The tolerance factor  $t$  was introduced by Goldschmidt [45] as a geometric criterion that determines the degree of stability and distortion of the crystal structure:

$$t = (R_A + R_O) / [\sqrt{2}(R_B + R_O)], \quad (2)$$

where  $R_A$  and  $R_B$  are the radii of cations in positions  $A$  and  $B$ , respectively;  $R_O$  is the ionic radius of oxygen. Values of tolerance factors  $t$  for the samples under study are shown in Table 2. In this work, the tolerance coefficient  $t$  was calculated taking into account the Shannon ionic radii for the corresponding coordination numbers (CN) ( $\text{O}^{2-}$  (CN = 6)  $R_{\text{O}^{2-}} = 1.40 \text{ \AA}$ ,  $\text{Nd}^{3+}$  (CN = 6)  $R_{\text{Nd}^{3+}} = 1.27 \text{ \AA}$ ,  $\text{W}^{6+}$  (CN = 6)  $R_{\text{W}^{6+}} = 0.6 \text{ \AA}$ ,  $\text{Ti}^{4+}$  (CN = 6)  $R_{\text{Ti}^{4+}} = 0.605 \text{ \AA}$ ). Shannon [46] did not provide the ionic radius of  $\text{Bi}^{3+}$  for coordination with CN = 12. Therefore, its value was determined from the ionic radius with CN = 8 ( $R_{\text{Bi}^{3+}} = 1.17 \text{ \AA}$ ) multiplied by an approximation factor of 1.179, then for  $\text{Bi}^{3+}$  (CN = 12) we got  $R_{\text{Bi}^{3+}} = 1.38 \text{ \AA}$ .

In addition to the results of structural studies, temperature dependences of the relative permittivity  $\epsilon$  and the loss tangent  $\text{tg}\sigma$  were obtained at various frequencies. Figure 3 shows the temperature dependences of the relative permittivity  $\epsilon(T)$  and the dielectric loss tangent for  $\text{Nd}^{3+}$   $\text{Bi}_{3-x}\text{Nd}_x\text{Ti}_{1.5}\text{W}_{0.5}\text{O}_9$  ( $x = 0.25, 0.5, 0.75, 1.0$ ) at a frequency from 100kHz to 1 MHz.

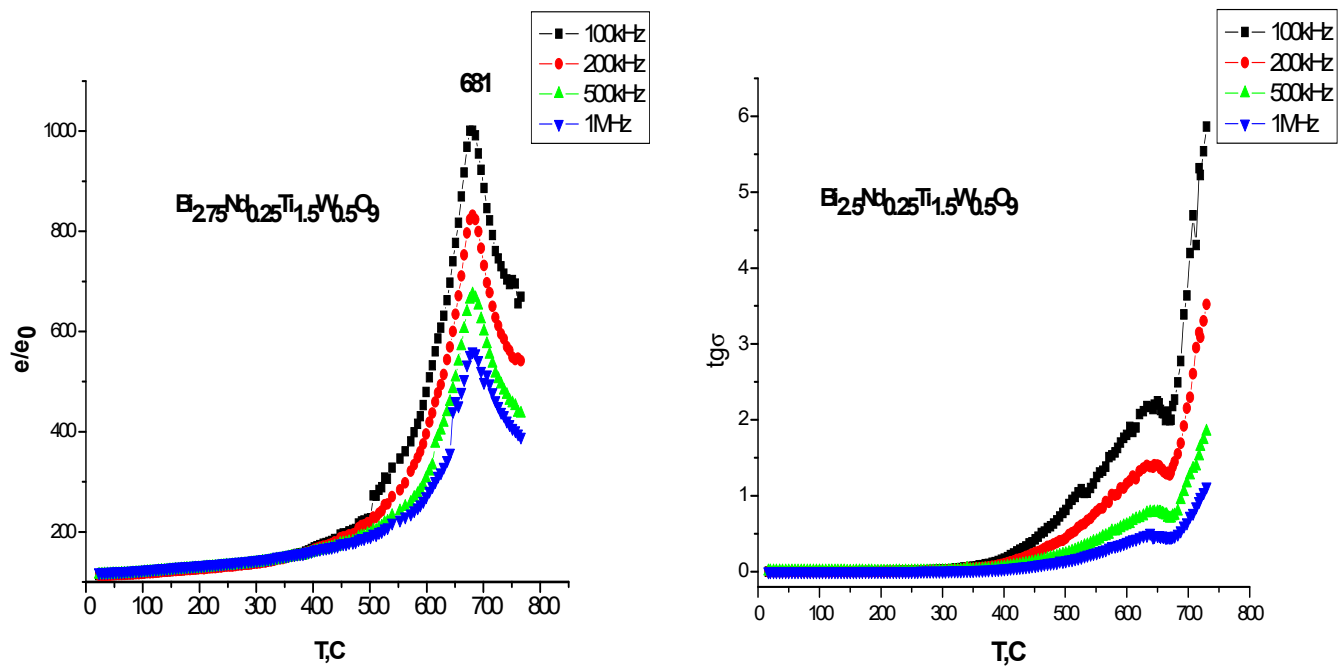


Figure 3. Cont.

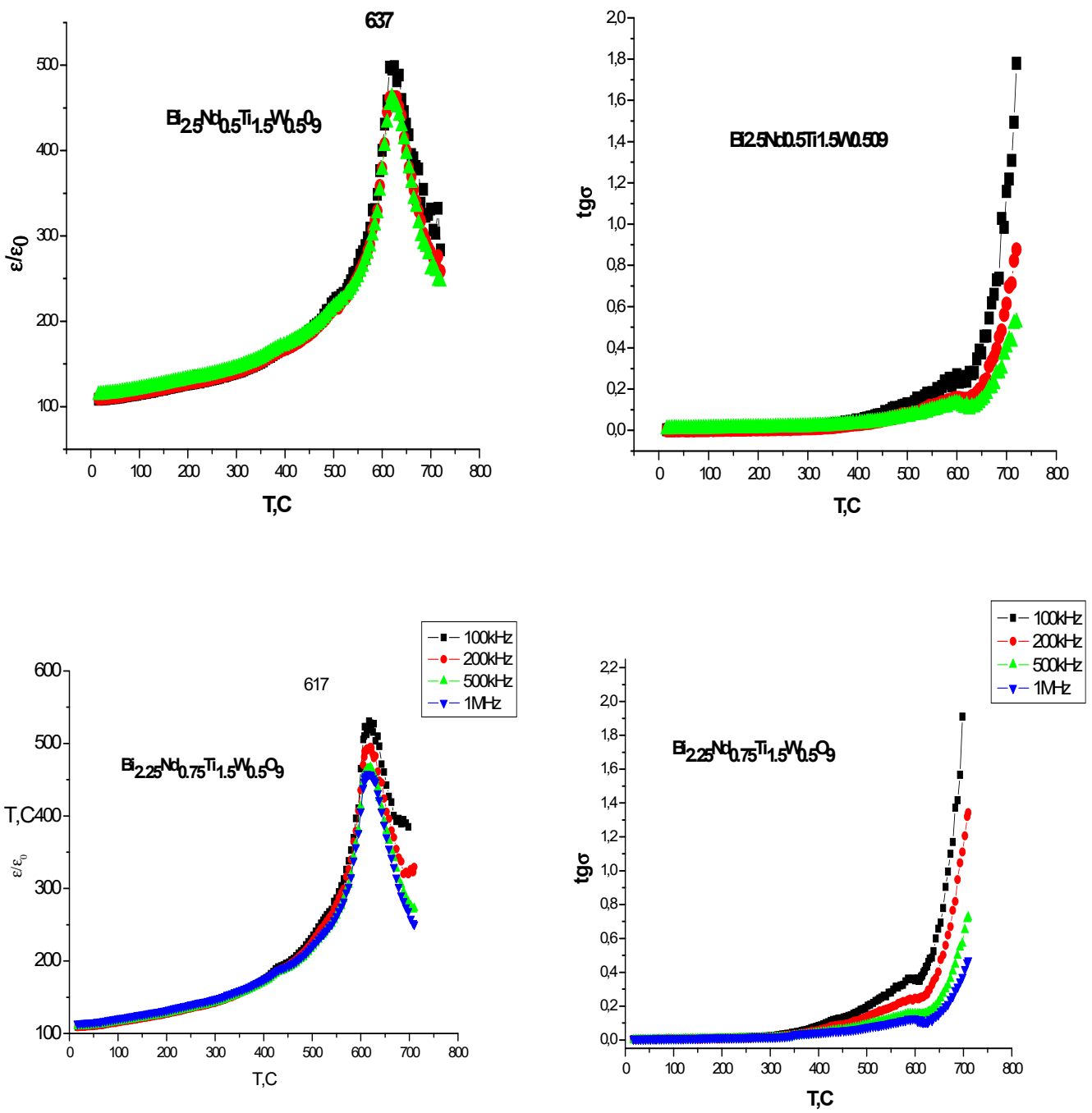
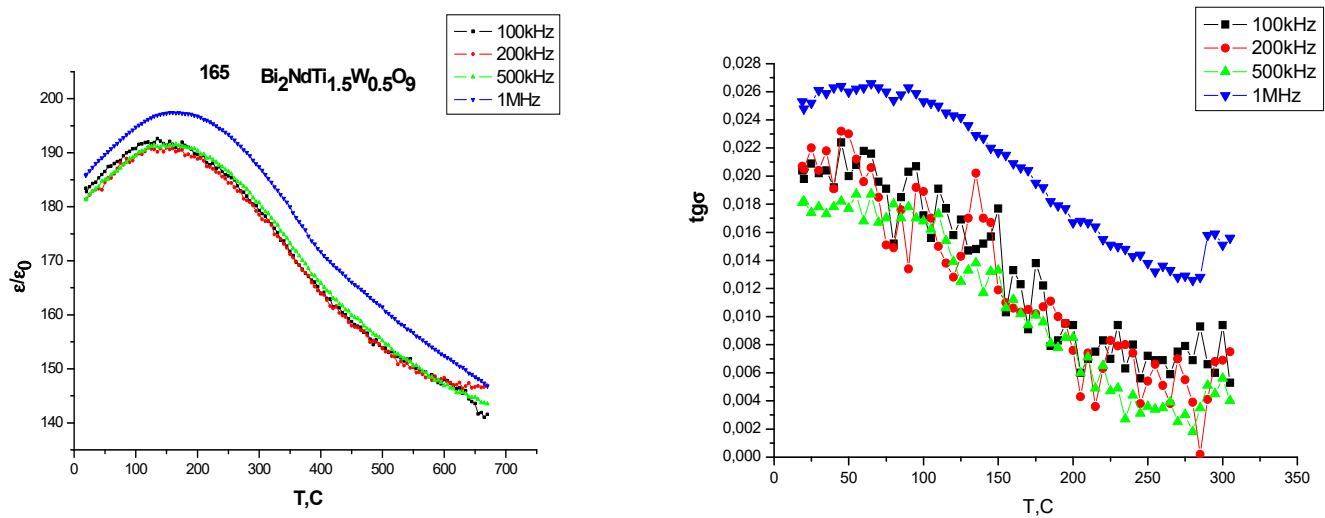


Figure 3. Cont.



**Figure 3.** Temperature dependences of the relative permittivity  $\varepsilon/\varepsilon_0$  and loss tangent  $\text{tg}\sigma$  for APs  $\text{Bi}_{3-x}\text{Nd}_x\text{Ti}_{1.5}\text{W}_{0.5}\text{O}_9$  ( $x = 0.25, 0.5, 0.75, 1.0$ ) at a frequency from 100 kHz to 1 MHz:  $\text{Bi}_{2.75}\text{Nd}_{0.25}\text{Ti}_{1.5}\text{W}_{0.5}\text{O}_9$ ,  $\text{Bi}_{2.5}\text{Nd}_{0.5}\text{Ti}_{1.5}\text{W}_{0.5}\text{O}_9$ ,  $\text{Bi}_{2.25}\text{Nd}_{0.75}\text{Ti}_{1.5}\text{W}_{0.5}\text{O}_9$ ,  $\text{Bi}_2\text{NdTi}_{1.5}\text{W}_{0.5}\text{O}_9$ .

For  $\text{Bi}_{3-x}\text{Nd}_x\text{Ti}_{1.5}\text{W}_{0.5}\text{O}_9$  ( $x = 0.25, 0.5, 0.75$ ), the  $\varepsilon(T)$  dependences are clearly pronounced. The intensity  $\varepsilon(T)$  in the range of 0.25–0.75 drops almost two times, while the dielectric loss decreases almost ten times. The temperature dependence of the relative permittivity  $\varepsilon/\varepsilon_0$  for the AP  $\text{Bi}_{3-x}\text{Nd}_x\text{Ti}_{1.5}\text{W}_{0.5}\text{O}_9$  ( $x = 1.0$ ) at a frequency from 100 kHz to 1 MHz has a strongly diffuse transition, which is usually typical of ferroelectric relaxors. The obtained values of the activation energy  $E_a$  of charge carriers in  $\text{Bi}_{3-x}\text{Nd}_x\text{Ti}_{1.5}\text{W}_{0.5}\text{O}_9$  ( $x = 0.25, 0.5, 0.75$ ) at frequency of 100 kHz are presented in Table 2.

The activation energy  $E_a$  was determined from the Arrhenius equation:

$$\sigma = (A/T)\exp[-E_a/(kT)], \quad (3)$$

where  $\sigma$  is the electrical conductivity,  $k$  is a Boltzmann's constant, and  $A$  is a constant,  $E_a$  is the activation energy. A typical dependence of  $\ln\sigma$  on  $1/(kT)$  (at a frequency of 100 kHz), which was used to determine the activation energies  $E_a$ , is shown in Figure 4 for the APs  $\text{Bi}_{3-x}\text{Nd}_x\text{Ti}_{1.5}\text{W}_{0.5}\text{O}_9$  ( $x = 0.25, 0.5, 0.75$ ). All three of these compounds  $\text{Bi}_{3-x}\text{Nd}_x\text{Ti}_{1.5}\text{W}_{0.5}\text{O}_9$  ( $x = 0.25, 0.5, 0.75$ ) have different temperature ranges in Figure 4, in which the activation energies  $E_a$  have significantly different behavior. If for the first two compounds  $x = 0.25, 0.5$ , three regions of the activation energy  $E_a$  of charge carriers are observed, then we observe only two regions for the compound  $x = 0.75$ . In the low-temperature range, the electrical conductivity is predominantly determined by impurity defects with very low activation energies of the order of a few hundredths of an electron-volt. For the  $\text{Bi}_{3-x}\text{Nd}_x\text{Ti}_{1.5}\text{W}_{0.5}\text{O}_9$  ( $x = 0.5, 0.75$ ) compounds, we do not observe a region with a clearly pronounced impurity conductivity.

At the same time, we observe for these compounds a decrease in the dielectric loss tangent and, as a consequence, a decrease in the conductivity. The decrease in the conductivity can be attributed to a decrease in oxygen vacancies.

Figure 5 shows the dependence of the unit cell parameters  $a$ ,  $b$ ,  $c$  on the parameter  $x$ . As seen from Figure 5, parameter  $a$  and  $b$  increase, while parameter  $c$  decreases for the entire series of compounds. It should also be noted that, despite the decrease in the thickness  $c'$  of the perovskite layer, the volume of the unit cell  $V$  increases. The change in the unit cell parameters  $a$ ,  $b$ ,  $c$ ,  $V$  and APs  $\text{Bi}_{3-x}\text{Nd}_x\text{Ti}_{1.5}\text{W}_{0.5}\text{O}_9$  ( $x = 0.25, 0.5, 0.75, 1.0$ ) is associated, among other things, with the difference in radii in the ions in position A, which have a dodecahedral layer, where position A is occupied by  $\text{Bi}^{3+}$  ions ( $R_{\text{Bi}^{3+}} = 1.38 \text{ \AA}$  [46]) and replaced by  $\text{Nd}^{3+}$  ions with a much smaller radius ( $R_{\text{Nd}^{3+}} = 1.27 \text{ \AA}$  [46]).

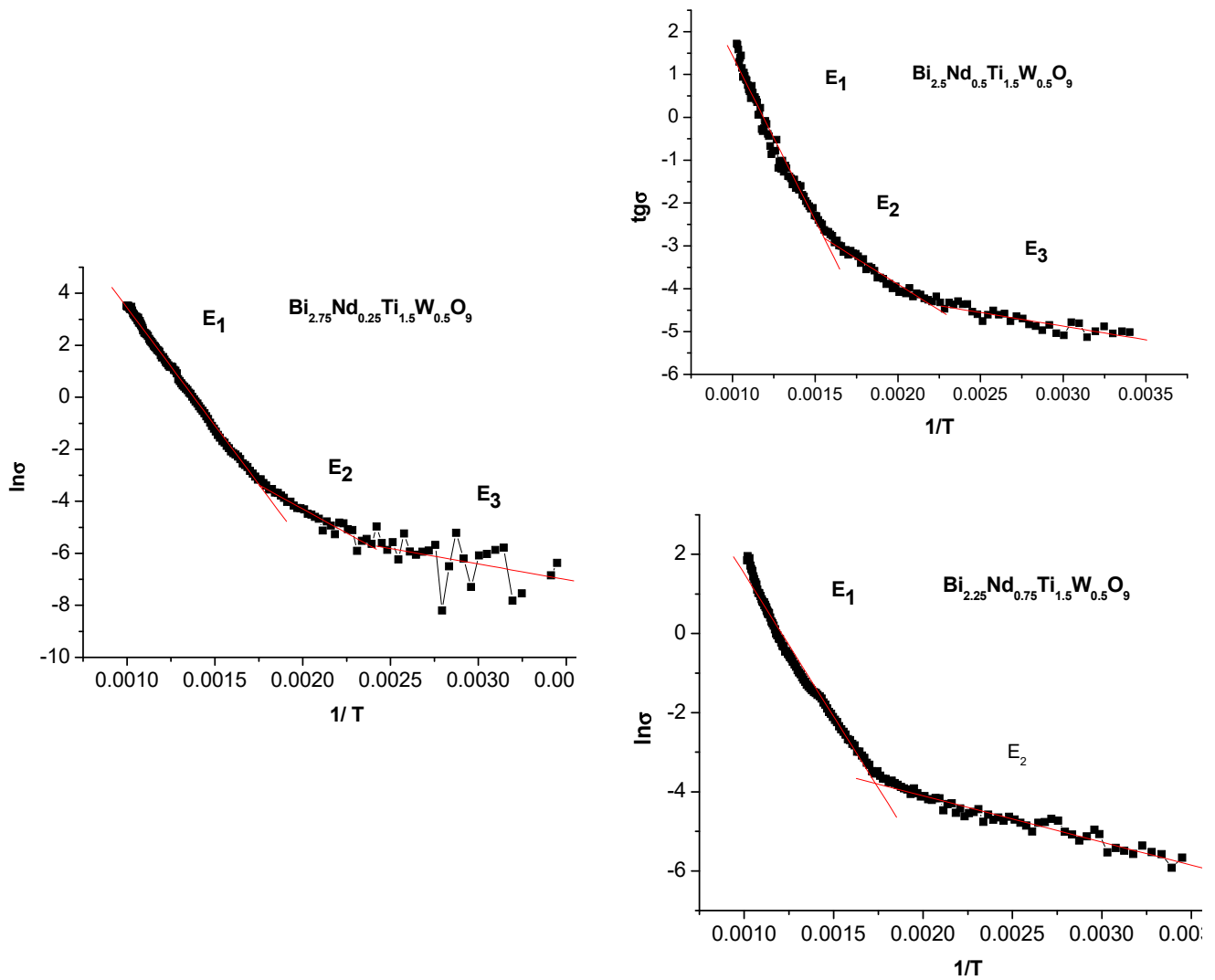


Figure 4. Dependence of  $\ln\sigma$  on  $1/T$  for the  $\text{Bi}_{3-x}\text{Nd}_x\text{Ti}_{1.5}\text{W}_{0.5}\text{O}_9$  ( $x = 0.25, 0.5, 0.75$ ) sample.

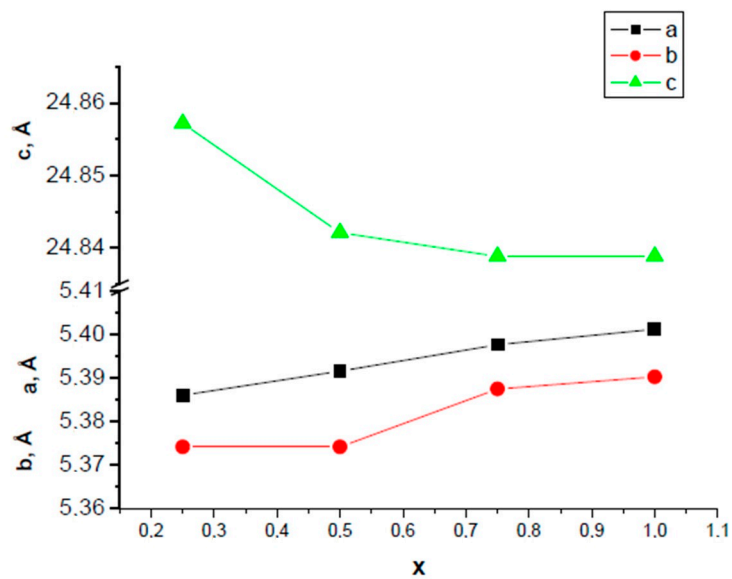


Figure 5. Dependences of the unit cell parameters  $a$ ,  $b$ ,  $c$  of the synthesized  $\text{Bi}_{3-x}\text{Nd}_x\text{Ti}_{1.5}\text{W}_{0.5}\text{O}_9$  ( $x = 0.25, 0.5, 0.75, 1.0$ ) on the parameter  $x$ .

It should be noted that the observed increase in the unit cell volume at  $x = 0.25$ – $1.0$  is associated only with a change in the unit cell parameters  $b$  and  $a$ , while the parameter  $c$  decreases. At the same time, if the parameter  $b$  changes almost linearly, then the parameter  $a$  has a non-linear dependence. It can be assumed that such a situation is possible if the neodymium ion has an ellipsoidal shape with a constant semi-major axis.

In Table 2, we can see the piezoelectric constant  $d_{33}$  for the  $\text{Bi}_{3-x}\text{Nd}_x\text{Ti}_{1.5}\text{W}_{0.5}\text{O}_9$  ( $x = 0.25, 0.5, 0.75$ ). For the  $\text{Bi}_{3-x}\text{Nd}_x\text{Ti}_{1.5}\text{W}_{0.5}\text{O}_9$  ( $x = 1.0$ ), the piezoelectric constant  $d_{33}$  could not be measured.

#### 4. Conclusions

Series of layered bismuth perovskite oxides  $\text{Bi}_{3-x}\text{Nd}_x\text{Ti}_{1.5}\text{W}_{0.5}\text{O}_9$  ( $x = 0.25, 0.5, 0.75, 1.0$ ) were synthesized by the solid-state method. The X-ray structural studies performed in our work showed that all the compounds obtained have single-phase with an orthorhombic crystal lattice (space group  $A2_1am$ ,  $Z = 36$ ). An analysis of the details of the AP-structure showed that an increase in the neodymium concentration  $x$  from 0.25 to 1.0 and a partial replacement of bismuth ions with neodymium ions lead to a decrease in the dielectric loss tangent and a decrease in  $\varepsilon/\varepsilon_0$ . For the entire series of synthesized compounds, the parameter  $c$  (thickness of the perovskite layer) decreases with an increase in neodymium cations. At the same time, the volume of the unit cell increases with decreasing  $c$  due to an increase in parameters  $a$  and  $b$ . Isovalent substitutions of  $\text{Bi}^{3+}$  ions by  $\text{Nd}^{3+}$  ions lead to a decrease in oxygen vacancies and leakage current and, accordingly, to a decrease in the dielectric loss tangent. Replacement of  $\text{Bi}^{3+}$  ions with  $\text{Nd}^{3+}$  ions, which have an ionic radius less than the ionic radius of bismuth, leads to a decrease in the Curie temperature  $T_C$ . This effect is observed only upon doping with neodymium ions. The temperature dependences  $\varepsilon/\varepsilon_0(T)$  in  $\text{Bi}_{3-x}\text{Nd}_x\text{Ti}_{1.5}\text{W}_{0.5}\text{O}_9$  ( $x = 0.25, 0.5, 0.75$ ) exhibit a high-temperature anomaly associated with the Curie temperature  $T_C$ , which corresponds to the transition from the paraelectric phase to ferroelectric. For  $\text{Bi}_{2.75}\text{Nd}_{0.25}\text{Ti}_{1.5}\text{W}_{0.5}\text{O}_9$  the piezoelectric constant is 10 pC/N and  $\text{tg}\sigma < 1$  at 1 MHz. Elements  $\text{Bi}_{3-x}\text{Nd}_x\text{Ti}_{1.5}\text{W}_{0.5}\text{O}_9$  ( $x = 0.25, 0.5, 0.75, 1.0$ ) of the synthesized series can become the basis for creating new lead-free piezo-ferroelectric materials.

**Author Contributions:** S.V.Z.—original draft preparation, writing—review and editing, investigation; I.A.P.—review and validation, conceptualization; Y.A.K.—X-ray investigation. All authors have read and agreed to the published version of the manuscript.

**Funding:** This research was funded by Southern Federal University, grant No. 21-19-00423.

**Acknowledgments:** The equipment of SFedU was used. The authors acknowledge the support by Southern Federal University, grant No. 21-19-00423 of the Russian Science Foundation.

**Conflicts of Interest:** The authors declare no conflict of interest.

#### References

1. Aurivillius, B. Mixed Bismuth Oxides with Layer Lattices: I. Structure Type of  $\text{CaBi}_2\text{B}_2\text{O}_9$ . *Arkiv Kemi* **1949**, *54*, 463–480.
2. Aurivillius, B. Mixed Bismuth Oxides with Layer Lattices: II. Structure Type of  $\text{Bi}_4\text{Ti}_3\text{O}_{12}$ . *Arkiv Kemi* **1949**, *58*, 499–512.
3. Aurivillius, B. Mixed Bismuth Oxides with Layer Lattices: III. Structure Type of  $\text{BaBi}_4\text{Ti}_4\text{O}_{15}$ . *Arkiv Kemi* **1950**, *37*, 512–527.
4. Smolensky, G.A.; Isupov, V.A.; Agranovskaya, A. New ferroelectric  $\text{PbBi}_2\text{Nb}_2\text{O}_9$ . *FTT* **1959**, 1969. (In Russian)
5. Ismayilzade. X-ray study of the structure of some new ferroelectrics with a layered structure. *Izv. AN SSSR* **1960**, *24*, 1198–1202. (In Russian)
6. Aurivillius, B. Ferroelectricity in the compound  $\text{BaBi}_4\text{Ti}_5\text{O}_{18}$ . *Phys. Rev.* **1962**, *12*, 6893–6896.
7. Subbarao, E.C. Crystal chemistry of mixed bismuth oxides with layer-type structure. *Am. Ceram. Soc.* **1962**, *45*, 166. [[CrossRef](#)]
8. Subbarao, E.C. Ferroelectricity in Mixed Bismuth Oxides with Layered-Type Structure. *Chem. Phys.* **1961**, *34*, 695.
9. Subbarao, E.C. A Family of Ferroelectric Bismuth Compounds. *Phys. Chem. Solids* **1962**, *23*, 665–676. [[CrossRef](#)]
10. Subbarao, E.C. Ferroelectricity in  $\text{BiTi}_3\text{O}_{12}$  and its solid solutions. *Phys. Rev.* **1961**, *122*, 804–807. [[CrossRef](#)]
11. Isupov, V.A. Crystal chemical aspects of the bismuth-containing layered compounds of the  $A_{m-1}\text{Bi}_2\text{B}_m\text{O}_{3m-3}$  type. *Ferroelectrics* **1996**, *189*, 211–217. [[CrossRef](#)]
12. Reznichenko, L.A.; Razumovskaya, O.N.; Shilkina, L.A.; Dergunova, N.V. On the relationship between the Curie temperature and the crystal-chemical characteristics of ions included in Bi-containing compounds. *Inorg. Mater.* **1996**, *32*, 474–481. (In Russian)

13. Isupov, V.A. Anomalies in the properties of layered ferroelectrics  $\text{Bi}_2\text{A}_{m-1}\text{B}_m\text{O}_{3m+3}$ . *Inorg. Mater.* **2006**, *421*, 353–1359. (In Russian)
14. Zubkov, S.V.; Vlasenko, V.G. Crystal structure and dielectric properties of layered perovskite-like solid solutions  $\text{Bi}_{3-x}\text{Y}_x\text{TiNbO}_9$  ( $x = 0.0, 0.1, 0.2, 0.3$ ) with high Curie temperature. *Phys. Solid State* **2017**, *59*, 2325. [[CrossRef](#)]
15. Zubkov, S.V.; Shevtsova, S.I. Crystal Structure and Dielectric Properties of Layered Perovskite-Like Solid Solutions  $\text{Bi}_{3-x}\text{Lu}_x\text{TiNbO}_9$  ( $x = 0, 0.05, 0.1$ ) with High Curie Temperature. *Adv. Mater.* **2020**, 173–182. [[CrossRef](#)]
16. Zarubin, I.A.; Vlasenko, V.G.; Shuvaev, A.T. Structure and dielectric properties of  $\text{Bi}_5\text{Sr}(\text{TiNb}_3)_{1-x}\text{B}_x\text{O}_{18}$  ( $0 < x \leq 0.25$ ; B = Sb, V, Re) layered perovskite-like solid solutions. *Inorg. Mater.* **2009**, *45*, 555.
17. Vlasenko, V.G.; Shuvaev, A.T.; Zarubin, I.A.; Vlasenko, E.V. Dielectric relaxation in layered oxides of the Aurivillius phase family. *Phys. Solid State* **2010**, *52*, 744. [[CrossRef](#)]
18. Gai, Z.G.; Zhao, M.L.; Su, W.B.; Wang, C.L.; Liu, J.; Zhang, J.L. Influences of ScTa co-substitution on the properties of Ultra-high temperature  $\text{Bi}_3\text{TiNbO}_9$ -based piezoelectric ceramics. *J. Electroceramic* **2013**, *31*, 143–147. [[CrossRef](#)]
19. Bekhtin, M.A.; Bush, A.A.; Kamentsev, K.E.; Segalla, A.G. Preparation and dielectric and piezoelectric properties of  $\text{Bi}_3\text{TiNbO}_9$ ,  $\text{Bi}_2\text{CaNb}_2\text{O}_9$ , and  $\text{Bi}_{2.5}\text{Na}_{0.5}\text{Nb}_2\text{O}_9$  ceramics doped with various elements. *Inorg. Mater.* **2016**, *52*, 557. [[CrossRef](#)]
20. Zhang, Z.; Yan, H.; Dong, X.; Wang, Y. Preparation and electrical properties of bismuth layer-structured ceramic  $\text{Bi}_3\text{NbTiO}_9$  solid solution. *Mater. Res. Bull.* **2003**, *38*, 241. [[CrossRef](#)]
21. Ando, A.; Kimura, M.; Sakabe, Y. Piezoelectric Properties of Ba and Ca Doped  $\text{SrBi}_2\text{Nb}_2\text{O}_9$  Based Ceramic Materials. *Appl. Phys.* **2003**, *42*, 520.
22. Hou, R.Z.; Chen, X.M. Synthesis and Dielectric Properties of Layer-structured Compounds  $\text{A}_{n-3}\text{Bi}_4\text{Ti}_n\text{O}_{3n+3}$  ( $A = \text{Ba}, \text{Sr}, \text{Ca}$ ) with  $n > 4$ . *Mater. Res.* **2005**, *20*, 2354. [[CrossRef](#)]
23. Hou, R.Z.; Chen, X.M.  $\text{La}^{3+}$  Substitution in Four-layers Aurivillius Phase  $\text{SrBi}_4\text{Ti}_4\text{O}_{15}$ . *Solid State Commun.* **2004**, *130*, 469. [[CrossRef](#)]
24. Noguchi, Y.; Miwa, I.; Goshima, Y.; Miyayama, M. Defect Control for Large Remanent Polarization in Bismuth Titanate Ferroelectrics Doping Effect of Higher-Valent Cations. *Appl. Phys.* **2000**, *39*, 1259. [[CrossRef](#)]
25. Yao, Y.Y.; Song, C.H.; Bao, P.; Su, D.; Lu, X.M. Doping effect on the dielectric property in bismuth titanate. *Appl. Phys.* **2004**, *95*, 3126. [[CrossRef](#)]
26. Newnham, R.E.; Wolfe, R.W.; Dorrian, J.F. Structural basis of ferroelectricity in the bismuth titanate family. *Mater. Res. Bull.* **1971**, *6*, 1029–1039. [[CrossRef](#)]
27. Moure, A.; Pardo, L.; Alemany, C.; Millan, P.; Castro, A. Piezoelectric ceramics based on  $\text{Bi}_3\text{TiNbO}_9$  from mechanochemically activated precursors. *Eur. Ceram.* **2001**, *21*, 1399. [[CrossRef](#)]
28. Zubkov, S.V.; Vlasenko, V.G.; Shuvaeva, V.A. Structure and dielectric properties of solid solutions  $\text{Bi}_7\text{Ti}_{4+x}\text{W}_x\text{Nb}_{1-2x}\text{O}_{21}$  ( $x = 0-0.5$ ). *Phys. Solid State* **2015**, *57*, 900.
29. Rajashekhar, G.; Sreekanth, T.; Ravikiran, U. Dielectric properties of Na and Pr doped  $\text{SrBi}_4\text{Ti}_4\text{O}_{15}$  ceramics. *Mater. Today* **2020**, *33*, 5467–5470.
30. Zubkov, S.V.; Vlasenko, V.G.; Shuvaeva, V.A.; Shevtsova, S.I. Structure and dielectric properties of solid solutions  $\text{Bi}_7\text{Ti}_{4+x}\text{W}_x\text{Ta}_{1-2x}\text{O}_{21}$  ( $x = 0-0.5$ ). *Phys. Solid State* **2016**, *58*, 42. [[CrossRef](#)]
31. Rizwana; Sarah, P. Dielectric, Ferroelectric and Piezoelectric Properties of  $\text{Sr}_{0.8}\text{Na}_{0.1}\text{Nd}_{0.1}\text{Bi}_4\text{Ti}_4\text{O}_{15}$  Prepared by Sol Gel and Solid State Technique. *Ferroelectrics* **2014**, *467*, 181–193. [[CrossRef](#)]
32. Fang, W.; Zhao, H.; Jia, T.; Fu, Q.; Xu, C.; Tao, H.; Weng, J.; Wang, S.; Ma, Z. Effects of La and Ni doping on ferroelectric and photocatalytic properties of Aurivillius  $\text{Bi}_7\text{Ti}_3\text{Fe}_3\text{O}_{21}$ . *Solid-State Electron.* **2021**, *186*, 108170. [[CrossRef](#)]
33. Dahake, K.; Jain, P.; Subohi, O. Impedance spectroscopy, dielectric, ferroelectric and electrical transport properties of Ba-doped  $\text{Bi}_3\text{TiNbO}_9$  ceramics. *J. Mater. Sci. Mater. Electron.* **2021**, *32*, 26770. [[CrossRef](#)]
34. Xi, J.; Xing, J.; Chen, H.; Zhang, F.; Chen, Q.; Zhang, W.; Zhu, J. Crystal structure and electrical properties of Li/Mn co-doped NBT-based Aurivillius type ceramics. *Alloys Compd.* **2021**, *868*, 159216. [[CrossRef](#)]
35. Rehman, F.; Li, J.-B.; Ahmad, I.; Jin, H.B.; Ahmad, P. Dielectric relaxation and electrical properties of  $\text{Bi}_{2.5}\text{Nd}_{0.5}\text{Nb}_{1.5}\text{Fe}_{0.5}\text{O}_9$  ceramics. *Mater. Chem. Phys.* **2019**, *226*, 100. [[CrossRef](#)]
36. Bartkowska, J.A.; Bochenek, D. Dielectric relaxation of manganese modified  $\text{Bi}_6\text{Fe}_2\text{Ti}_3\text{O}_{18}$  Aurivillius type ceramics. *Arch. Metall. Mater.* **2019**, *64*, 221.
37. Cheng, Z.X.; Wang, X.L. A way to enhance the magnetic moment of multiferroic bismuth Ferrite. *J. Phys. D* **2010**, *43*, 242001. [[CrossRef](#)]
38. Sengupta, P.; Sadhukhan, P.; Ray, A.; Mal, S.; Singh, A.; Ray, R.; Bhattacharyya, S.; Das, S. Influence of activation energy on charge conduction mechanism and giant dielectric relaxation of sol-gel derived  $\text{C}_3\text{H}_7\text{NH}_3\text{PbBr}_3$  perovskite; Act as high performing UV photodetector. *Alloys Compd.* **2021**, *892*, 162216. [[CrossRef](#)]
39. Zdorovets, M.; Kozlovskiy, A.; Arbut, A.; Tishkevich, D.; Zubar, T.; Trukhanov, A. Phase transformations and changes in the dielectric properties of nanostructured perovskite-like LBZ composites as a result of thermal annealing. *Ceram. Int.* **2020**, *46*, 14460. [[CrossRef](#)]
40. Long, C.; Chang, Q.; Wu, Y.; He, W.; Li, Y.; Fan, H. New layer-structured ferroelectric polycrystalline materials,  $\text{Na}_{0.5}\text{Nd}_x\text{Bi}_{4.5-x}\text{Ti}_4\text{O}_{15}$ : Crystal structures, electrical properties and conduction behaviors. *Mater. Chem. C* **2015**, *3*, 8852.

41. Sengupta, P.; Sadhukhan, P.; Ray, A.; Ray, R.; Bhattacharyya, S.; Das, S. Temperature and frequency dependent dielectric response of  $C_3H_7NH_3PbI_3$ : A new hybrid perovskite. *J. Appl. Phys.* **2020**, *127*, 204103. [[CrossRef](#)]
42. Kozlovskiy, A.L.; Kenzhina, I.E.; Zdorovets, M.V.; Saiymova, M.; Tishkeviche, D.I.; Trukhanov, S.V.; Trukhanov, A.V. Synthesis, phase composition and structural and conductive properties of ferroelectric microparticles based on  $ATiO_x$  ( $A = Ba, Ca, Sr$ ). *Ceram. Int.* **2019**, *45*, 17236. [[CrossRef](#)]
43. Zubkov, S.V. Structure and dielectric properties of solid solutions  $Bi_{7-2x}Nd_{2x}Ti_4NbO_{21}$  ( $x = 0.0, 0.2, 0.4, 0.6, 0.8, 1.0$ ). *Adv. Dielectr.* **2021**, *11*, 2160018. [[CrossRef](#)]
44. Kraus, W.; Nolze, G. *PowderCell for Windows, Version 2.3*; Federal Institute for Materials Research and Testing: Berlin, Germany, 1999.
45. Goldschmidt, V.M. *Geochemische Verteilungsgesetze der Elemente*; Norske: Oslo, Norway, 1927.
46. Shannon, R.D. Revised Effective Ionic Radii and Systematic Studies of Interatomic Distances in Halides and Chalcogenides. *Acta Crystallogr. Sect. A* **1976**, *32*, 751. [[CrossRef](#)]